Peer-reviewed version available at *Cells* **2020**, *9*, 1267; doi:10.3390/cells9051267

Review

A Structural View at SARS-CoV-2 RNA Replication Machinery: RNA Synthesis, Proofreading and Final Capping

Maria Romano±1, Alessia Ruggiero±1, Flavia Squeglia±1, Giovanni Maga2, Rita Berisio1*

1 Affiliation 1; Institute of Biostructures and Bioimaging, IBB, CNR, Naples, Italy,
2 Affiliation 2; Institute of Molecular Genetics, IGM, CNR, Pavia, Italy,
* Correspondence: rita.berisio@cnr.it;
± These authors contributed equally to this work
corresponding author, R.B.

Abstract: COVID19 is a current pandemic disease due to the novel coronavirus SARS-CoV-2. The scientific community mounted a strong response by accelerating research and innovation, and rapidly setting the basis to the understanding of molecular determinants of the disease for the development of targeted therapeutic interventions. The replication of the viral genome within the infected cells is a key step of SARS-CoV2 life cycle. It is a complex process involving the action of several viral and host proteins in order to perform RNA polymerization, proofreading and final capping. This review provides an update of structural and functional data on key actors of the replicatory machinery of SARS-CoV-2, filling the gaps in the current availability of structural data using homology modelling. Moreover, learning from similar viruses, we collect literature data to reconstruct the pattern of interactions among protein actors of the SARS-CoV-2 RNA polymerase machinery. In this pattern, an important role is played by co-factors, like Nsp8 and Nsp10, not only as allosteric activators but also as molecular connectors holding the entire machinery together to enhance the efficiency of RNA replication.

Keywords: SARS-CoV-2; COVID19; RNA replication; protein structure; infectious disease

1. Introduction

The current outbreaking COVID-19 (Coronavirus Disease-2019) is a respiratory disease caused by a novel enveloped, positive-sense, single-stranded RNA betacoronavirus, denoted as SARS-CoV-2. In December 2019, a cluster of patients in the Chinese city of Wuhan was diagnosed with a pneumonia of unknown etiology. Its causative agent, SARS-CoV-2, has caused at the time of writing over 2.400.000 confirmed cases and 165.000 fatalities worldwide. The significant infectivity, the fact that about 15%-20% of infected people develop pneumonia and the relevant lethality in risk groups such as elderly people, immunodeficiency patients and people affected by chronic respiratory and heart diseases, make SARS-CoV-2 infection a serious global health threat. Consistently, on January 30th the World Health Organization (WHO) has declared the situation a public health emergency of international concern and last March 11nd, a pandemic threat. The scientific community is promptly responding to the emergency by heavily focusing on accelerating research and innovation, as witnessed by the copious recent literature, setting the basis to the understanding of molecular determinants of disease and the development of targeted therapeutic interventions [1-3]. These ground breaking studies have shown that SARS-CoV-2 shares 79.5% of its genome to SARS-CoV [1], sufficiently divergent from SARS-CoV to be considered a new human-infecting betacoronavirus [3]. Genome sequence analysis revealed SARS-CoV-2 phylogenetic relationships with bat-derived SARS-like coronaviruses, suggesting a zoonotic origin [1]. However, much of what we can infer about the

biology of SARS-CoV-2 comes from previous studies on the SARS-CoV. Starting from these data, the molecular mechanisms underneath evolution, adaptation, and spread of this virus warrant urgent investigation.

SARS-CoV-2 gets into the cell through the recognition by the spike glycoprotein, present on the surface of the virus envelope, of the Angiotensin Converting Enzyme 2 (ACE2) receptors, as previously observed for SARS-CoV [4,5]. Recently, another human receptor, CD147, has been identified as a possible route of viral entrance, again mediated by the spike protein [6]. After attachment, a human protease cleaves and activates the spike protein [7], in an event that allows SARS-CoV-2 to enter the cells by endocytosis or direct fusion of the viral envelope with the host membrane [8,9]. Once inside the cell, the infecting RNA acts as a messenger RNA (mRNA), which is then translated by host ribosomes to produce the viral replicative enzymes, which generate new RNA genomes and the mRNAs for the synthesis of the components necessary to assemble the new viral particles. SARS-CoV-2 replication is a complex process which involves RNA synthesis, proofreading and capping. On analogy with other viruses, this process is likely to actively involve many host proteins, which are exploited by the virus for a more efficient replication [10-12]. Understanding molecular mechanisms at guiding replication of this coronavirus is essential to develop therapeutic tools to neutralize SARS-CoV-2. Here, we review structural information, mostly obtained through homology modelling based on the available structures for other coronaviruses, on main protein actors of SARS-CoV-2 RNA replication and transcription.

2. Organization of SARS-CoV-2 genome

Like other coronaviruses, SARS-CoV-2 has a positive-sense single-stranded genomic RNA, approximately 30 kb in length [13], among the largest known RNA genomes. Its genome contains 14 open reading frames. Of these, ORF1a and ORF1ab encode replicase polyprotein 1a (PP1a) and polyprotein 1ab (PP1ab) (Figure 1). The largest polyprotein PP1ab encode non-structural proteins (Nsp1-16), which form the complex replicase machinery. This includes enzyme activities that are rare or absent in other families of positive-stranded (+) RNA viruses [14]. At the 3′ end, the viral genome encodes four structural proteins (Spike, Envelope, Membrane, Nucleocapsid) which are components of the mature virus and play a crucial role in viral structure integrity or, as in the case of the spike protein, for viral entry in the host [4-6]. Interspersed among the structural genes, the 3′ end of the genome also contains nine putative ORFs for accessory factors [15] (Figure 1).

Preprints (www.preprints.org) | NOT PEER-REVIEWED | Posted: 29 April 2020 doi:10.20944/preprints202004.0510.v1

Peer-reviewed version available at Cells 2020, 9, 1267; doi:10.3390/cells9051267

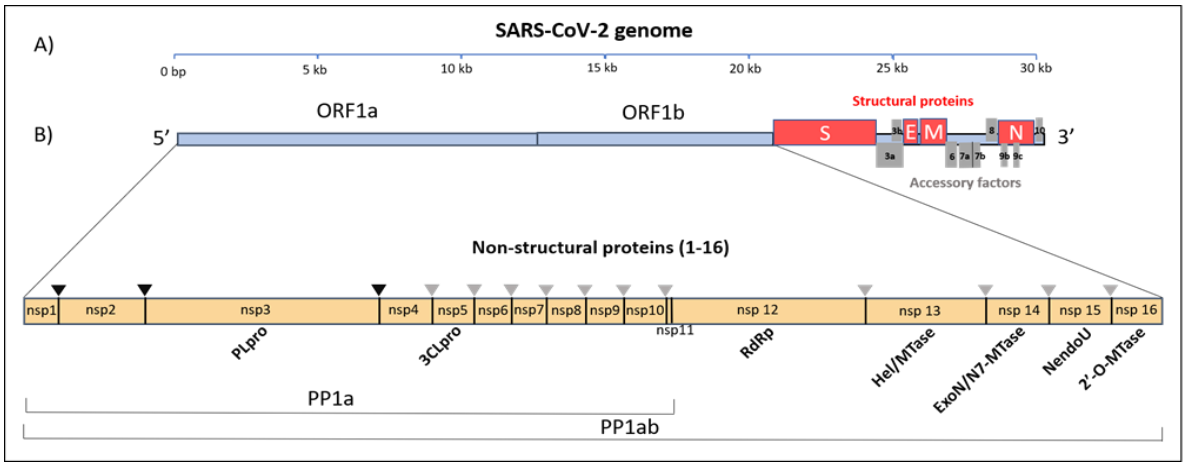

Figure 1. SARS-CoV-2 19 polycistronic genome. (A) Genome of SARS-COV-2 organized in individual ORFs. (B) PP1ab encode 16 Nsps; the black and grey triangles indicate the cleavage sites of the protease PLpro and 3CLpro, respectively. Names of confirmed and putative functional domains in the Nsp proteins are also indicated.

3. A structural view at SARS-CoV-2 RNA replicatory machinery

3.1. RNA machinery as a whole: Nsp interaction pattern

The viral RNA replication machinery of SARS-CoV-2 involves an array of functional proteins from the N- to C-termini of the polyprotein PP1ab (Figure 1). These include the essential RNA-dependent RNA polymerase (RdRp, Nsp12) [16] and the zinc-binding helicase (HEL, Nsp13) [17] and a number of other enzymatic function related to viral RNA modification, such as mRNA capping (Nsp14, Nsp16), RNA proofreading (Nsp14) [18-20], and uridylate-specific endoribonuclease activity (NendoU, Nsp15) [21,22]. Activity of these enzymes is further regulated by the association with other non structural proteins (Nsp7–Nsp10) that are likely necessary to achieve all the replication and the transcription processes [23-25]. All of these protein subunits likely associate, as observed for other nidoviruses, into a replication transcription enzyme complex anchored to membranes derived from the host cell ER [26,27], that drives the synthesis of new genome molecules and also subgenomic (sg) messenger RNAs (mRNAs) [28]. Table 1 reports all structural information hitherto available for non-structural proteins from SARS-CoV-2 and its homologs, together with their proposed functions.

Table 1. Available structural information on putative SARS-CoV-2 RNA replication machinery actors.

Target	Function	PDB Code [Reference]	Source	Seqid (%)
Nsp7	Cofactor of Nsp12	1YSY (85) [104]; 2KYS [105]; 2AHM (in complex with Nsp8) [106]; 6NUR (complex with Nsp8 e Nsp12) [39]	SARS-CoV	98.8
Nsp8	Cofactor of Nsp12	2AHM (complex with Nsp7) [106]; 6NUR (complex with Nsp7 e Nsp12) and 6NUS (complex with Nsp12) [39]	SARS-CoV	97.5
Nsp9	RNA binding protein	6W4B, 6W9Q, 6WC1 [107]; 1QZ8 [108]; 1UW7 [109]	SARS-CoV-2 SARS-CoV	100 97.4
Nsp10	Cofactor of Nsp16 and Nsp14	6W61, 6W75 6W4H (complex with Nsp16); 2XYR, 2XYV, 2XYQ (complex with Nsp16)[88]; 3R24 (complex with Nsp16) [87]; 5NFY (complex with Nsp14) [68]; 5C8S, 5C8T, 5C8U (complex with Nsp14) [61]; 2GA6 [102]	SARS-CoV-2 SARS-CoV	100 98.5

Nsp12	RNA-directed RNA polymerase	6M71 and 7BTF (in complex with Nsp7 and Nsp8 [40]; 7BV1 (complex with Nsp7 and Nsp8) and 7BV2 (complex with Nsp7 and Nsp8, RNA template/primer and Remdesivir, [45]; 6NUS (complex with Nsp8) and 6NUR (complex with Nsp7 and Nsp8) [39]	SARS-CoV-2 SARS-CoV	100 96.4
Nsp13	Helicase, 5′ triphosphatase	6JYT [32]; 5WWP [98]	SARS-CoV, MERS-CoV	99.8 72.2
Nsp14	3′-5′ exoribonuclease, ExoN; Guanine-N7 methyltransferase , N7 MTase	5C8S, 5C8U, 5C8T (complex with Nsp10) [61]; 5NFY (complex with Nsp10) [68]	SARS-CoV	95.1 94.9
Nsp15	NendoU, Uridylate-specific endoribonuclease	6W01, 6VWW [110]; 2H85 [111]; 2RHB [112]	SARS-CoV-2 SARS-CoV	100 88.0
Nsp16	2'-O-ribose methyltransferase	6W4H, 6W75, 6W61 (complex with Nsp10); 2XYR, 2XYV, 2XYQ (complex with Nsp10) [88]; 3R24 (complex with Nsp10) [87]; 5YN5 (complex with Nsp10).	SARS-CoV-2 SARS-CoV MERS-CoV	100 93.5 66.1

Literature data on possible interactions among individual actors of the RNA polymerase machinery of SARS-CoV-2 are still limited. However, based on data of highly homologous proteins from either SARS-CoV (sequence identity > 88%) or mouse hepatitis virus (MHV) (sequence identity > 40%, Table S1), we reconstituted the likely pattern of interactions among the Nsp proteins constituting the RNA replication/transcription machinery (Figure 2). Among these, we predict that Nsp12 and Nsp8 play a central role in the assembly of the entire RNA polymerase replicative machinery. Nsp12, the RNA-dependent RNA polymerase is the key enzyme mediating the synthesis of all viral RNA molecules [29]. Biochemical studies have proved that Nsp12 from SARS-CoV exhibits low processive RNA synthesis *in vitro*, as it requires the presence Nsp7 and Nsp8 to bind nucleic acid and perform an efficient RNA synthesis [23,24]. The direct association between Nsp8 and Nsp12 has been reported in several coronaviruses and it is a feature likely shared by most, if not all, coronaviruses [30,31]. We also predict that Nsp12 of SARS-CoV-2 is able to interact with Nsp13 helicase, based on studies of the highly homologous Nsp12 and Nsp13 from SARS-CoV (96.4 and 99.8 % sequence identity, respectively). Indeed, Nsp12 of SARS-CoV can enhance the helicase activity of Nsp13 through a direct protein-protein interaction [32]. The positive regulation of Nsp13 by Nsp12 is an important event in viral replication. Indeed, mutation of specific conserved residues of Nsp13 can either negatively impact or block replication of the arterivirus equine arteritis virus (EAV)[33,34]. Finally, on analogy with SARS-CoV, Nsp12 is most likely able to associate with Nsp14 [24], Nsp5 and Nsp9 [35] (Figure 2).

Nsp8 and Nsp7/Nsp8 complex can also bind and enhance the endoribonuclease NendoU activity of MERS-CoV Nsp15 *in vitro* [36]. This result agrees with previous evidence showing that Nsp15 from MHV colocalizes and interacts *in vivo* with Nsp8 and Nsp12 [37]. However, whether Nsp15 belongs to the RNA replication machinery is still an open question. Finally, Nsp8 deletion or disruption of the protease cleavage site between Nsp7 to Nsp9, necessary to correctly process the corresponding proteins, both result in impaired RNA synthesis and lethal phenotype in MHV [38]. Altogether, these findings identify the Nsp12-Nsp8 complex as a key hub for the viral replication machinery (Figure 2).

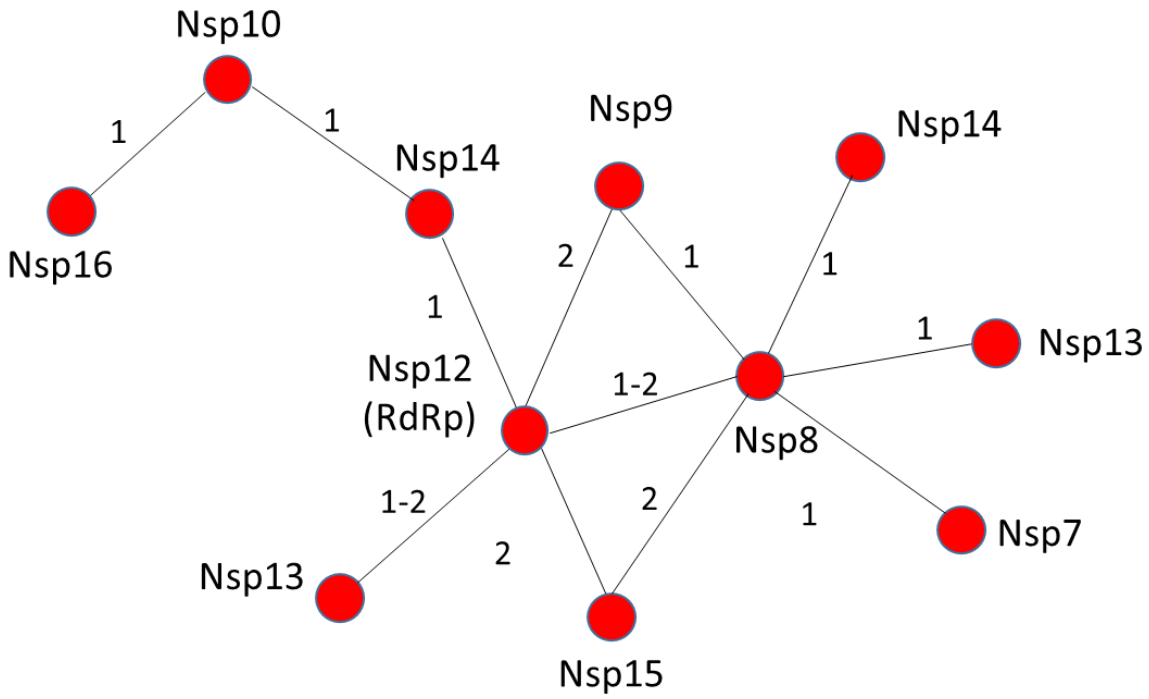

Figure 2. Nsp12 and Nsp8 are a hub for interactions among actors of the RNA replication machinery: Predicted pattern of interactions based on the available literature data. The numbers 1 and 2 on the strings are referred to SARS-CoV and MHV, respectively.

3.2. RNA polymerization requires Nsp12 and cofactors Nsp7, Nsp8

SARS-CoV-2 RNA polymerization relies on a main polymerase, Nsp12, also denoted as RNA-dependent RNA polymerase, RdRp. Nsp12 is a large enzyme (932 residues) characterized by two conserved domains: the NiRAN and the polymerase domains (Figure 3A). The structure of SARS-CoV Nsp12 bound to the Nsp7 and Nsp8 cofactors has been recently determined using cryo-EM [39]. During the preparation of this manuscript, also the structure of SARS-CoV-2 Nsp12 has been reported [40]. Consistent with the high sequence identity between the Nsp12 form SARS-CoV and SARS-CoV-2 (94%), the two structures are nearly identical, as indicated by their root mean square deviation of 0.8 Å for 1078 Cα atoms [40]. In both structures, Nsp12 is complexed with the two co-factors Nsp7 and Nsp8 (Figure 3B). The observed interactions in the complex structure Nsp12-Nsp8-Nsp7 are compatible with a previous work addressing the impact of residues of Nsp7 and Nsp8 on their interactions with Nsp12 [24].

Preprints (www.preprints.org) | NOT PEER-REVIEWED | Posted: 29 April 2020 doi:10.20944/preprints202004.0510.v1

Peer-reviewed version available at Cells 2020, 9, 1267; doi:10.3390/cells9051267

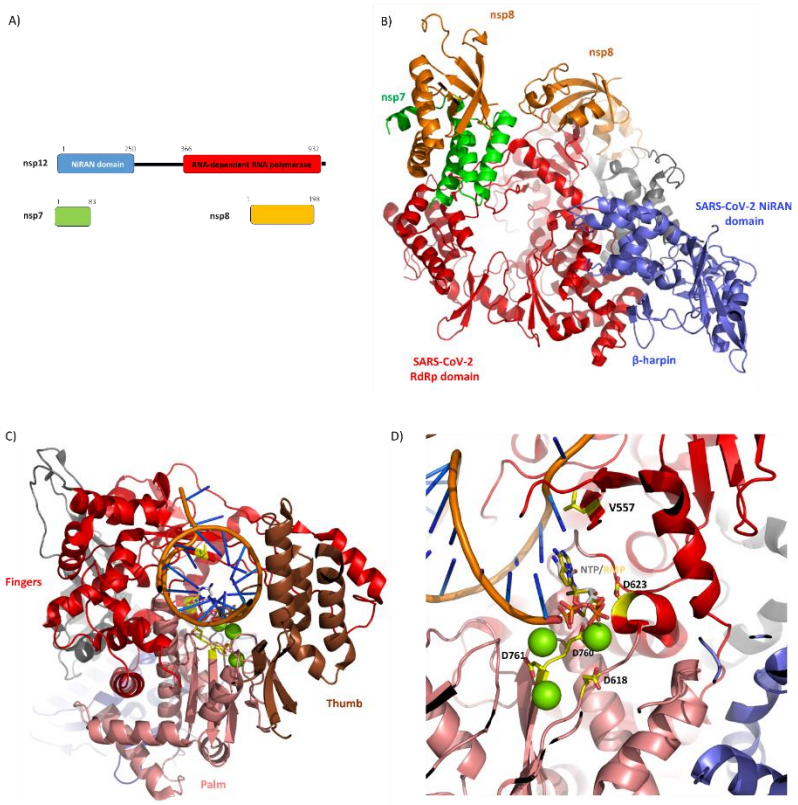

Figure 3. SARS-CoV-2 Nsp12-Nsp7-8 complex. A) Domain organization of Nsp12, with its Nsp7 and Nsp8 cofactors, according to Pfam. B) Cartoon representation of Nsp12 SARS-CoV-2 bound to Nsp7 and Nsp8 cofactors (PDB code 7BTF). C) Model of SARS-CoV-2 elongation complex. The positions of the RNA template/primer and of the divalent cations were obtained from the structural alignment of the complex in panel A with the elongation complex from SARS-CoV-2 (PDB code 7BV2), while the position of NTP was obtained from the alignment with the polymerase of norovirus (PDB code 3H5Y). The three subdomains of the polymerase domain, fingers (residues 366-581 and 621-679), palm (residues 582-620 and 680-815), and the thumb (residues 816-920) are shown in red, salmon and brown, respectively. D) A zoom of the catalytic site showing the position of the incoming NTP, Remdesivir monophosphate (RMP) (in stick) and divalent cations (as green spheres). The conserved Asp residues playing a key role in the NTP and Mg2+ binding and Val557 (involved in Remdesivir resistance) are shown as yellow sticks.

The N-terminal domain of Nsp12, that has been shown to be essential for viral growth in both equine arteritis virus (EAV) and SARS-CoV [41], is conserved in all nidoviruses endowed with nucleotidylation activity. Therefore, it is named NiRAN from Nidovirus RdRp-Associated Nucleotidyltransferase (Figure 3A,B) [41]. The structure of the NiRAN domain was only partially described in the structure of SARS-CoV Nsp12, whereas it is fully complete in the last released structure of SARS-CoV-2 Nsp12-Nsp7-Nsp8 complex [40]. Overall, this domain forms is characterized by an $\alpha+\beta$ fold composed of eight α helices and a five stranded β-sheet (Figure 3B). In addition, an N-terminal β-hairpin (residues 29-50) interacts with the palm subdomain of the RdRp domain (Figure 3B) [40]. This information provides structural tools to understand the functional role of the NiRAN domain in Nsp12. Indeed, although the exact role of this domain is not fully clear, structural similarity analyses using DALI suggest that the NiRAN domain of SARS-CoV-2 Nsp12 displays structural features of kinase-like folds [39]. Indeed, using DALI we identified two kinases as the most similar structures, the Serine/Threonine kinase PRP4 homolog (PDB code 6PJJ, DALI Z=10.5, RMSD=2.8 Å, seqid 15%) and Tyrosine-protein kinase JAK1 (PDB code 6C7Y, DALI Z=10, RMSD=2.8 Å, seqid 11%) [42]. Given the importance of the NiRAN domain in viral growth [41], this structural observation suggests a further tool for drug development using kinase inhibitors.

The RNA polymerase C-terminal domain of Nsp12 (residues 366-920) from SARS-CoV-2 adopts a conformation that has been described as a cupped right hand, constituted of finger, palm and thumb subdomains [39,40] (Figure 3C). Biochemical and structural studies of polymerases from other viruses, e.g. poliovirus and foot-and-mouth disease virus, have defined the catalytic cycle of the RNA polymerase as a multistep process composed of successive steps [43,44]. Catalytic residues can be identified in SARS-CoV-2, upon alignment with poliovirus RNA polymerase, whose catalytic residues are known, with the two aspartic acids Asp618 and Asp760 (Figure S1). Consistently, the D760A mutant of SARS-CoV Nsp12 is unable to synthetize RNA [24]. Together with these two aspartic acids, also Asp623 and Asp761 are involved in the recognition of the NTP triphosphate and divalent cations, respectively [39,40]. The recent crystal structure of SARS-CoV-2 Nsp12-Nsp7-Nsp8 has confirmed that both Asp760 and Asp761 are involved in coordination of the two important magnesium ions at the catalytic center (Figure 3D). Importantly, a key initiation step is the addition of the first one or two nucleoside triphosphates (NTP) onto a primer, to form a stable and processive elongation complex [43,44]. The structure of the elongation complex of SARS-CoV-2 contains 14 bases in the template strand and 11 bases in the primer strand. This double-stranded RNA helix contacts all of the three Nsp12 subdomains (finger- palm-thumb, Figure 3C). Most of protein-RNA interactions are mediated with the RNA phosphate-ribose backbones, with many interactions directly to 2′-OH groups, thus providing a basis to distinguish RNA from DNA [45]. Notably, the position of the RNA primer is nearly superimposable to that obtained for the well characterized poliovirus [43,46] (Figure 3D, S1). Also residues involved in RNA binding and composing the catalytic active site are highly conserved (Figure 3, S1), thus suggesting a similar mechanism of RNA replication. It is interesting to note that apo and complexed Nsp12 are almost identical, with an RMSD of 0.5 Å, thus suggesting that SARS-CoV-2 Nsp12 does not require a conformational switch upon ligand binding. This hypothesis well agrees with the high processivity of viral RNA polymerases [44], since no extra energy is required to switch the enzyme conformation towards activation.

Although sequence identity of Nsp12 with RdRP from the Ebola virus (EBOV) is quite poor (16%), structural analysis indicates the conservation of the polymerase active site. Consistently, Remdesivir, the nucleotide inhibitor of the EBOV RdRP has been recognized as a promising antiviral drug against a wide array of RNA viruses including filoviruses, arenaviruses, paramyxoviruses, and other coronaviruses with divergent RdRp, such as SARS-CoV, MERS-CoV, bat CoV, and the new SARS-CoV-2 strains [47-52], in cultured cells, mice and nonhuman primate models [47,53,54]. Remdesivir is a prodrug, which is metabolized into its active form (GS-441524) that causes a decrease in viral RNA production [47] (Figure 4). The compound has a 1′-cyano group, which provides potency and selectivity toward viral RNA polymerases, and a monophosphate promoiety to enhance intracellular metabolism into the active triphosphate metabolite [55] (Figure 4). Remdesivir triphosphate is able to inhibit EBOV replication with half maximal effective concentrations (EC50) in the submicromolar range [47], by blocking viral RNA synthesis [47]. The mechanism of inhibition is a delayed chain termination of nascent viral RNA, as described for several viral RdRP, including EBOV, MERS, Nipah (NIV) and Respiratory syncytial virus RSV [47,56-58]. In all cases, Remdesivir triphosphate inhibits transcription by competing with the incorporation of natural NTP counterparts [56,58]. This finding has been recently corroborated for SARS-CoV-2 by the determination of the structure of Nsp12-Nsp7-Nsp8 in complex with RNA template/primer and Remdesivir [45] (Table 1). This structure has shown that Remdesivir monophosphate (RMP) is covalently incorporated at the 3′ end of the primer strand [45]. As shown in Figure 3D, this position fully overlaps with the +1 position of a natural NTP. Consistently, it was previously shown for MHV and SARS-CoV [48] that a mutation of a conserved valine residue of Nsp12, corresponding to V557L in SARS-CoV-2, confer low-level resistance to Remdesivir, it impairs fitness and attenuate virulence. This mutation is located in proximity to the NTP binding site of Nsp12 [45] (Figure 3D).

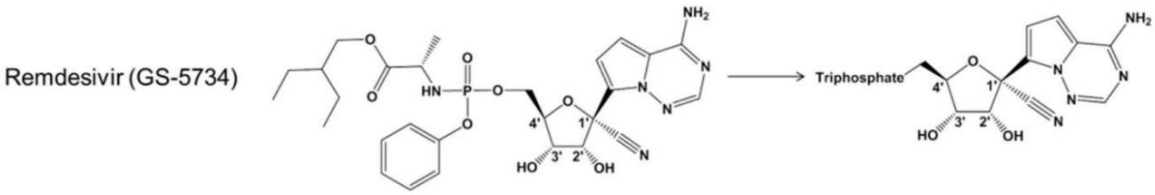

Figure 4. Chemical structures of Remdesivir (GS-5734) and of its pharmacologically active nucleoside triphosphate NTP (GS-441524).

Significantly, a recent study revealed that Remdesivir and Chloroquine (an old antimalarial drug) were highly effective in the control of SARS-CoV-2 *in vitro* [50]. From the clinical point of view, Remdesivir is being used in a small number of SARS-CoV-2 positive patients as "compassionate use" based on the patients' worsening clinical status. One of the first cases in the USA is responding well to the nucleoside analogue with an immediate improving after intravenous injection [59]. Nevertheless, it is not yet approved for general use and clinical trials are currently underway to determine its safety and efficacy [60]. Structural based improvements of this drug may constitute a valid tool to enhance its specificity and efficiency against coronaviruses.

3.3. RNA proofreading through the bifunctional protein Nsp14, involved in a unique RNA proofreading mechanism and mRNA capping, and cofactor Nsp10

Nsp14 of SARS-CoV-2 contains two domains with different functions, as identified by the PFAM database (Figure 5A). The N terminal domain (ExoN) is endowed with exoribonuclease activity and includes three conserved motifs: motif I (DE), II (E) and III (D). Due to this feature, Nsp14 is included, as a "DEED outlier" into the superfamily of DEDD exonucleases [61,62], which embrace enzymes with proofreading activity [62,63]. In line with this observation, ExoN knockout mutants of SARS-CoV and Murine Hepatitis Virus (MHV) were shown to accumulate a high number of mutations [64,65]. The carboxy-terminal part of Nsp14, containing (N7 guanine)-methyl transferase activity, is involved in the viral mRNA cap synthesis. The RNA final cap has several important biological roles in viruses, as it is critical for the stability of mRNAs, for their translation and to evade the host immune response. Indeed, uncapped RNA molecules are degraded in cytoplasmic granular compartments and may be detected as 'non-self' by the host, therefore triggering innate immune responses [66,67].

Preprints (www.preprints.org) | NOT PEER-REVIEWED | Posted: 29 April 2020 doi:10.20944/preprints202004.0510.v1

Peer-reviewed version available at Cells 2020, 9, 1267; doi:10.3390/cells9051267

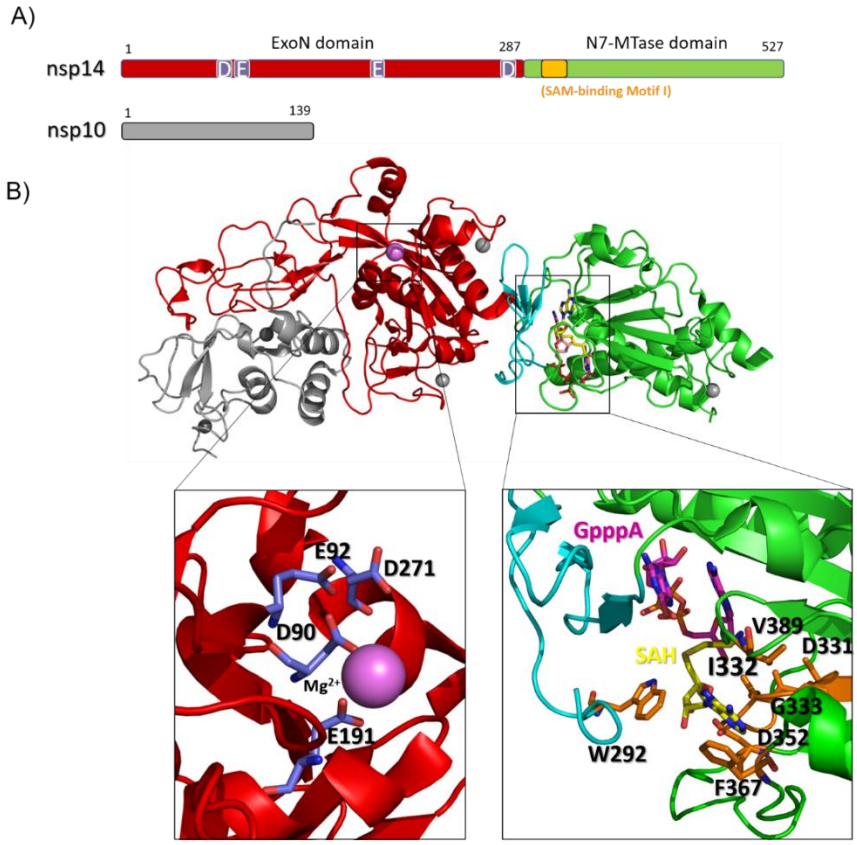

Figure 5. Homology model of SARS-CoV-2 Nsp14-Nsp10 complex. A) Domain organization of Nsp14 and Nsp10; B) Cartoon representation of the homology model of the complex, computed with MODELLER using the structure of its homolog from SARS-CoV (5c8s) as a template. Zinc atoms are shown as grey and a Mg2+ ion as magenta spheres. Zooms of the catalytic sites are shown in the insets. Catalytic residues of the ExoN domain (left inset) are shown as blue sticks, those of the N7-MTase domain (right inset) are shown as orange sticks; the cap-precursor GpppA (pink), a SAH (demethylated form of SAM) ligand (yellow) and the SAM-binding motif residues (orange) are also reported in stick representation.

A homology model of the complex between Nsp14 and Nsp10 of SARS-CoV-2 is reported in Figure 5B, based on structures of homologous proteins of SARS-CoV [61,68] (Table S1). In this complex, the co-factor Nsp10, composed of a helical domain and an irregular β-sheet region followed by a loop region at its C-terminus, forms multiple interactions with the ExoN domain of Nsp14, likely stabilizing it. Consistently, SAXS experiments of Nsp14 from SARS-CoV in the absence of Nsp10 show large conformational changes in the N terminus of Nsp14, which affect the overall shape of the exonuclease fold [68]. Importantly, the interaction with Nsp10 strongly affect the nucleolytic activity of SARS-CoV Nsp14, which is enhanced up to 35-fold [69].

The ExoN domain of Nsp14 presents an α/β fold as the other members of the DEDD exonuclease superfamily [70]. It is composed by a central twisted β-sheet formed by five β -strands. These, are flanked by α-helices, with the exception of the strand β3 (Figure 5B) [61,68]. Based on the structural alignment with SARS-CoV, catalytic residues of ExoN domain of SARS-CoV-2 Nsp14 include the DEED residues Asp90, Glu92, Glu191, Asp272 (Figure 5). A structural alignment using DALI shows that this domain is structurally similar to *E. coli* RNase T and to RNase AS from *M. tuberculosis*, two exonucleases involved in RNA maturation through 5′ processing [71,72]. Similar to these exonucleases, alanine substitution of the four catalytic residues of ExoN, which coordinate a Mg^{2+} ion (Figure 5B), gives a significant reduction of the viral RNA synthesis [64,71-74]. Altogether, these data suggest that like Nsp12, Nsp14 has a crucial role in SARS-CoV-2 replication through its ExoN domain,

as it is involved in maintaining the integrity of the SARS-CoV-2 RNA genome, preventing and repairing mutations [65,75]. In this context, susceptibility of EBOV to Remdesivir also involves the proofreading exoribonuclease, Nsp14 [48]. For EBOV RNA polymerase, the incorporation of the nucleotide analogue at position n causes inhibition of RNA synthesis predominantly at position n+5 [57,58], whereas in the case of MERS, RNA synthesis arrest occurs at position n+3, with these three nucleotides likely protecting the inhibitor from excision by the viral 3′–5′ exonuclease activity [58]. In both cases, delayed chain-termination could be due to inhibitor-induced structural changes of the newly synthesized double stranded RNA [76,77]. Importantly, a mutant lacking ExoN was significantly more sensitive to Remdesivir, suggesting that this nucleoside analogue, once incorporated into viral RNA, can be removed by the exoribonuclease activity of Nsp14 during proofreading [48,78]. Therefore, nucleoside analogues that effectively inhibit viral RNA replication must either evade detection by the exonuclease or outcompete exonuclease activity [79]. In this direction, chemical modifications of the nucleoside analogues to skip recognition by Nsp14, or simultaneous inhibition of Nsp12 and Nsp14, would provide a synergistic action in the inhibition of RNA synthesis and be a powerful strategy against SARS-CoV-2.

A flexible hinge region consisting of a loop and three strands (as cyan in Figure 5B) separates the ExoN domain from the N7-MTase domain of Nsp14 and is highly conserved across CoVs. This region allows lateral and rotational movements of the two domains to coordinate the two different enzymatic activities of Nsp14 (Figure 5B) [62]. Following this hinge region, the N7-MTase domain is an (N7 guanine)-methyl transferase involved in RNA capping, which operates by demethylating its co-enzyme S-adenosyl methionine (SAM). This domain shows unique structural features, as it displays an atypical fold, different from the canonical Rossmann fold of the virus RNA MTase [68,80]. In addition, it does not belong to any of the classes of SAM-dependent MTases [81-83]. Indeed, a typical Rossmann fold embeds a central core of β-sheets composed of seven parallel β-strands, with at least three a-helices on each side [80]. Differently, the β sheet of the N7-MTase domain of Nsp14 is formed by five β -strands instead of seven (Figure 5B). SARS-CoV Nsp14-Nsp10 crystal structure [61], together with alanine scanning mutagenesis [84] and cross-linking experiments, revealed two clusters of residues that are key for the N7-MTase activity (Figure 5B) [84-86]. The first cluster is a canonical SAM-binding motif I (DxGxPxG/A) and includes Asp331, Gly333, Pro335 and Ala337 (Figure 5B), where SAM is the methyl donor in the (N7 guanine)-methyl transferase reaction catalyzed by Nsp14. A second cluster forms a pocket that holds the GTP of the mRNA cap structure in close proximity of the methyl donor SAM (Figure 5B). The binding mode of the functional ligands, the cap-precursor guanosine-P3-adenosine-5′,5′-triphosphate (GpppA) and the product of SAM demethylation, S-adenosyl Homocysteine (SAH), occurs with no significant structural changes of the enzyme [61]. These studies have contributed to shed light on the mechanism of RNA cap formation, which also involves several other protein actors, as detailed below.

3.4. SARS-CoV-2 capping machinery involves Nsp13, Nsp14, Nsp16 and the co-factor Nsp10

3.4.1. RNA cap synthesis in coronaviruses

mRNAs of coronaviruses are protected at their 5′ ends by a cap structure consisting of an N7-methylated GTP molecule linked to the first transcribed nucleotide by a 5′–5′ triphosphate bond. Given the importance of RNA capping for mRNA stability and as a mechanism to evade the host immune response, RNA-capping machineries are an attractive target for antiviral-drug design. In Coronaviruses, the cap synthesis involves, apart from the N7-MTase domain of Nsp14 described above, several enzymes and the co-factor Nsp10 (Figure 6). The mRNA cap (^{m7}GpppN-RNA) is composed by a 7-methylguanosine (^{m7}G) linked to the 5′-nucleoside (N) of the RNA chain through a triphosphate bridge (ppp). The process begins with the hydrolysis of the 5′γ-phosphate of the nascent RNA chains (pppN-RNA) by an RNA 5′-triphosphatase, the Nsp13 helicase [17]. Subsequently, a GTase, still unidentified, transfers a GMP molecule to the 5′-diphosphate of the RNA chains (ppN-RNA), leading to the formation of GpppN-RNA. Then, the cap structure is methylated at the N7

position of the guanosine by the C-terminal N7-MTase domain of Nsp14, forming cap-0 (^{m7}GpppN-RNA), using SAM as a methyl donor. Finally, Nsp16 (SAM)-dependent 2'-O-methyltransferase activity promotes the addition of a methyl group on the ribose 2'-O position of the first transcribed nucleotide to form cap-1 (^{m7}GpppNm-RNA) [87,88] (Figure 6). In the last steps, the cofactor Nsp10 acts as an allosteric activator [87,88].

3.4.2. Start of mRNA capping by the multi-functional Nsp13 helicase

Helicases are versatile NTP-dependent enzymes, that are widespread in all kingdoms of life including (+) RNA viruses with genome greater than 7 kb. They are classified into six superfamilies (SF1 to SF6) and are known to be critically involved in several processes connected to nucleic acid metabolism [89]. Helicases are required for unwinding of dsDNA and/or dsRNA substrates, for displacing proteins bound to nucleic acid or remodelling DNA or RNA secondary structures and for translocating along double-strand nucleic acid without unwinding [34]. Sequence conservation analysis shows that Nsp13 of SARS-CoV-2 belongs to SF1 superfamily and shares many structural features with the eukaryotic Upf1 helicase, a key factor in nonsense-mediated mRNA decay in cells [90]. Learning from other coronaviruses, Nsp13 exhibits multiple enzymatic activities, which include not only the hydrolysis of NTPs required in the capping mechanism (Figure 6), but also unwinding of RNA duplexes with 5'-3' directionality and the RNA 5'-triphosphatase activity [91,92]. Additionally, RNA unwinding activity is stimulated by the interaction with the RdRP Nsp12 [93]. Nsp13 is highly conserved in all coronaviruses and is a key enzyme in viral replication [94,95], two observations which make it a promising target for antiviral therapies [34]. In this context, a potent non-competitive inhibitor (SSYA10-001) blocks viral replication by inhibiting the unwinding activity of the helicase Nsp13 [96], not only in SARS-CoV but also for two other coronaviruses, MHV and MERS-CoV [97].

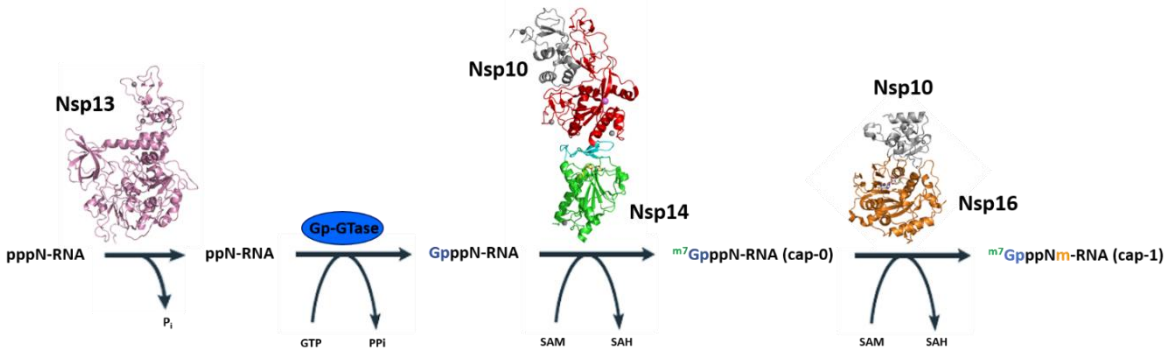

Figure 6. The mRNA cap synthesis process in SARS-CoV-2. The process is performed by the sequential action of four enzymes: Nsp13 (pink), a still unknown GTase, Nsp14 (red) and Nsp16 (orange). The presence of the co-factor Nsp10 (grey) is fundamental for the activity of the last two enzymes.

Nsp13 of SARS-CoV-2 shares the same structure as that of SARS-CoV [32], given the extremely high conservation of protein sequences (Table S1), and consists of five domains which fold in a triangular pyramid shape (Figure 7B). A similar organization was observed for MERS helicases [98]. Three domains named 1A and 2A and the 1B domain are arranged to form the triangular base, leaving the remaining two domains, the N-terminal Zinc binding domain (ZBD) and the stalk domain, at the apex of the pyramid (Figure 7B). Mutagenesis and structural alignments demonstrated that the 1B, 1A and 2A domains are responsible for NTP activity and nucleic acid binding, whereas other functional information structural about the structural coordination of these five domains in helicase activity have been deduced through the H/D exchange assays. As explained above, the activity of Nsp13 is enhanced by Nsp12 through a direct interaction, with the interaction region on Nsp13 mapped on the ZBD domain and the 1A domain [32]. Given the high sequence conservation of these two proteins, their association can be considered a common feature across CoV [32].

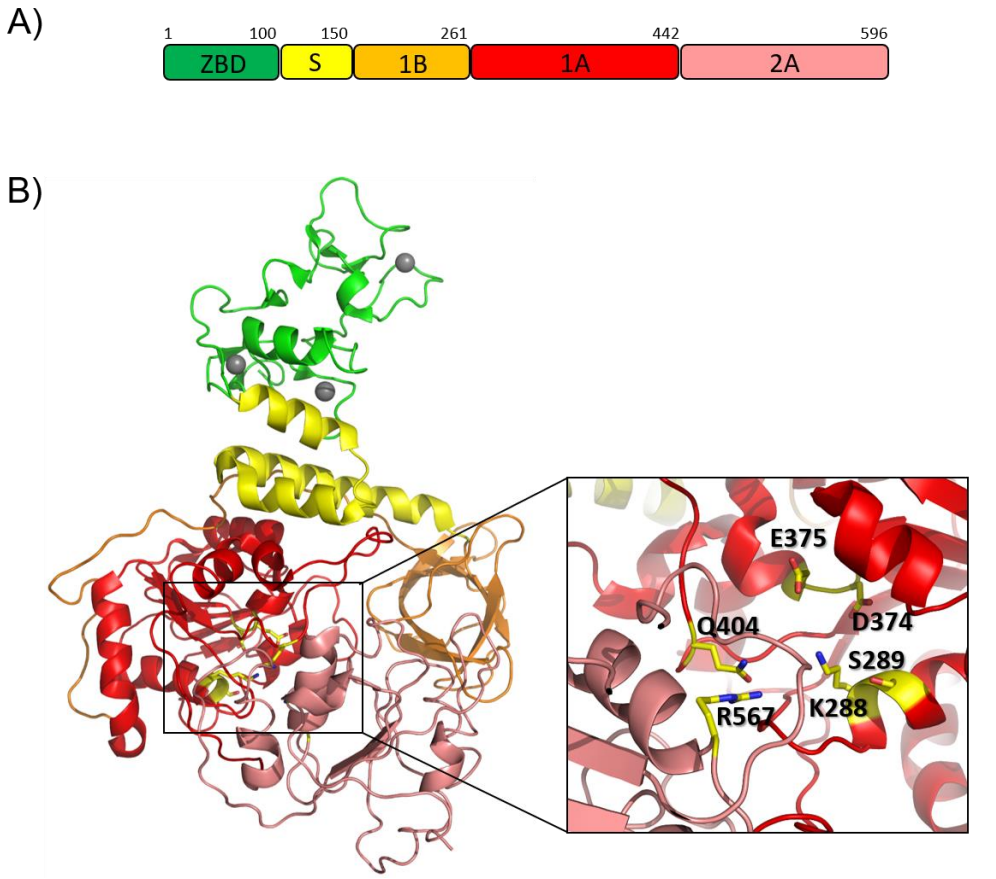

Figure 7. SARS-CoV-2 Nsp13 helicase. A) Domain organization of SARS-CoV-2 Nsp13. B) Cartoon representation of the homology model of SARS-CoV-2 Nsp13, based on the crystallographic structure of the SARS-CoV (PDB code 6JYT). The colours of the protein domains are indicated in panel A (ZBD-green, stalk-yellow, 1B-orange, 1A-red and 2A-salmon). Three zinc atoms are shown as grey spheres. In the inset, the key conserved residues responsible for NTP hydrolysis are drawn in stick.

3.4.3. End of mRNA capping by 2′-O-Methyl Transferase Nsp16 and Nsp10, an allosteric activator and a molecular connector?

Several x-ray structures of Nsp16 are deposited in the PDB, including those from SARS-CoV, MERS-CoV and more recently of SARS-CoV-2 (Table 1). In all of these structures, Nsp16 is complexed with the cofactor Nsp10 and presents a similar topological organization [87,99]. In particular, Nsp16 possesses the typical fold of the class I MTase family, comprising a seven-stranded β sheet flanked by α helices with the characteristic reversed β hairpin at the carboxyl end of the sheet (β6- β7) (Figure 8) [83]. The catalytic site cleft of Nsp16 contains the conserved K-D-K-E catalytic tetrad, which is peculiar of SAM-dependent 2′O-methyltranferases. Specifically, the four residues Lys46, Asp130, Lys170 and Glu203 are predicted to be catalytic (Figure 8) [83]. In addition, a conserved SAM-binding pocket is located at the C-terminal end of strands β1 and β2, as in the case of other SAM-dependent MTases [100] (Figure 8). Two zinc ions were identified as bound to two zinc finger regions and found to be indispensable for the binding of the RNA chains in a nonselective manner (Figure 8) [101-103].

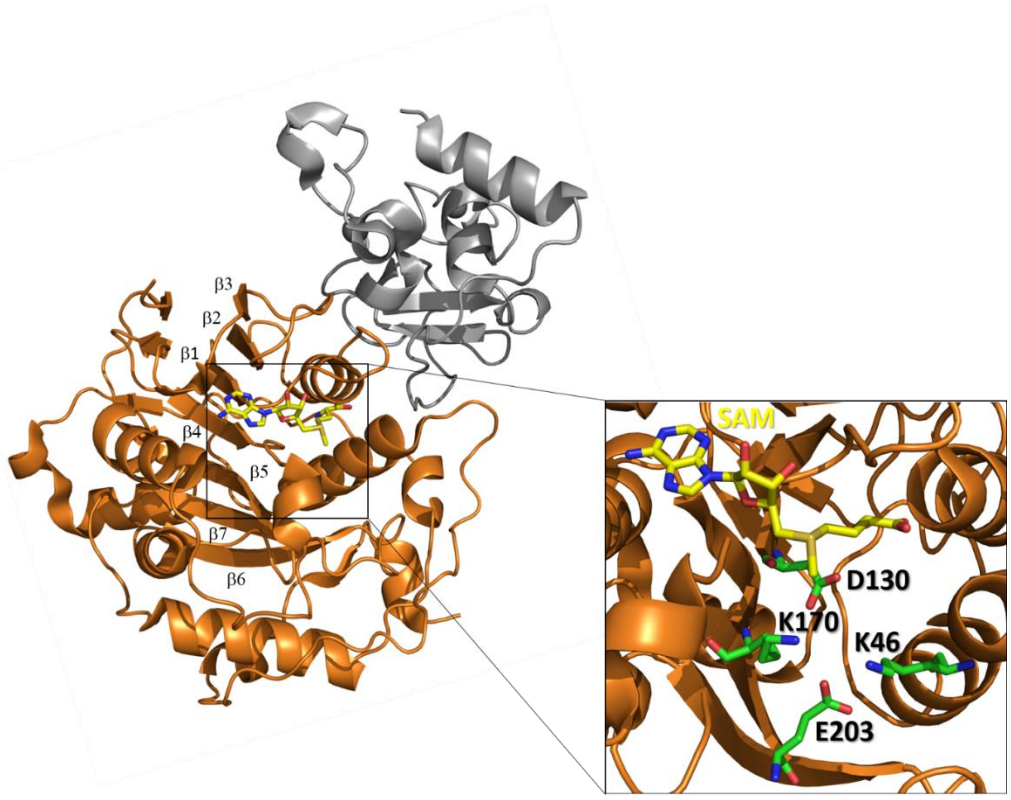

Figure 8. Structure of the SARS-CoV-2 Nsp10-Nsp16 complex. Cartoon representation of the crystal structure complex (PDB code 6W4H) of Nsp16 (orange) in complex with Nsp10 (grey). The inset shows the catalytic site of Nsp16. Catalytic residues (green) and the SAM ligand (yellow) are shown in stick representation.

As shown in the case of SARS-CoV, Nsp16 needs to interact with Nsp10 to become active [87]. Indeed, SARS CoV Nsp16 alone has low affinity for both m7GpppA-RNA and m7GpppA cap analogue, and the interaction between the two proteins increases RNA-binding affinity [87]. Similar results were observed for MERS CoV Nsp16/Nsp10 complex [99].

As previously discussed, the cofactor Nsp10 plays a similar activating role for Nsp14, as demonstrated for SARS-CoV [69]. Therefore, we explored the possibility of the formation of a ternary complex Nsp10/Nsp14/Nsp16 by verifying the compatibility of binding of Nsp14 and Nsp16 to Nsp10 (See caption to Figure 9 for details). As shown in Figure 9, interacting regions on Nsp10 with Nsp14 and Nsp16 are perfectly complementary, thus allowing for a simultaneous interaction of Nsp10 with both Nsp14 and Nsp16. This finding suggests the likely scenario of Nsp10 working not only as an allosteric activator of the two enzymes but also as a molecular connector, joining together in space three catalytic sites (Figure 9). As shown in Figure 9, a ternary complex Nsp10-Nsp14-Nsp16 would keep close in space the proofreading site of Nsp14 with the two catalytic sites responsible for capping on Nsp14 and on Nsp16. This ternary complex is likely only a part of a large RNA polymerase complex, which is further hold together by the known interactions between the ExoN domain of Nsp14 and Nsp12 [24] and between Nsp13 and Nsp12 [32], although fine details of these interactions are still unknown (Figure 9). In the case of a nucleotide mismatch, the nascent RNA strand can be efficiently moved from Nsp12 to the ExoN site of the RNA polymerase complex for excision (Figure 9). Final capping is then provided by the sequential activities of close-in-space enzymes. Namely, the Nsp13 helicase, the GTase and then the N7-MTase activity of Nsp14 and the 2′-OMTase activity of Nsp16 (Figure 9), thus completing the nascent RNA strand with the cap1 structure at its 5′ end.

Preprints (www.preprints.org) | NOT PEER-REVIEWED | Posted: 29 April 2020 doi:10.20944/preprints202004.0510.v1

Peer-reviewed version available at Cells 2020, 9, 1267; doi:10.3390/cells9051267

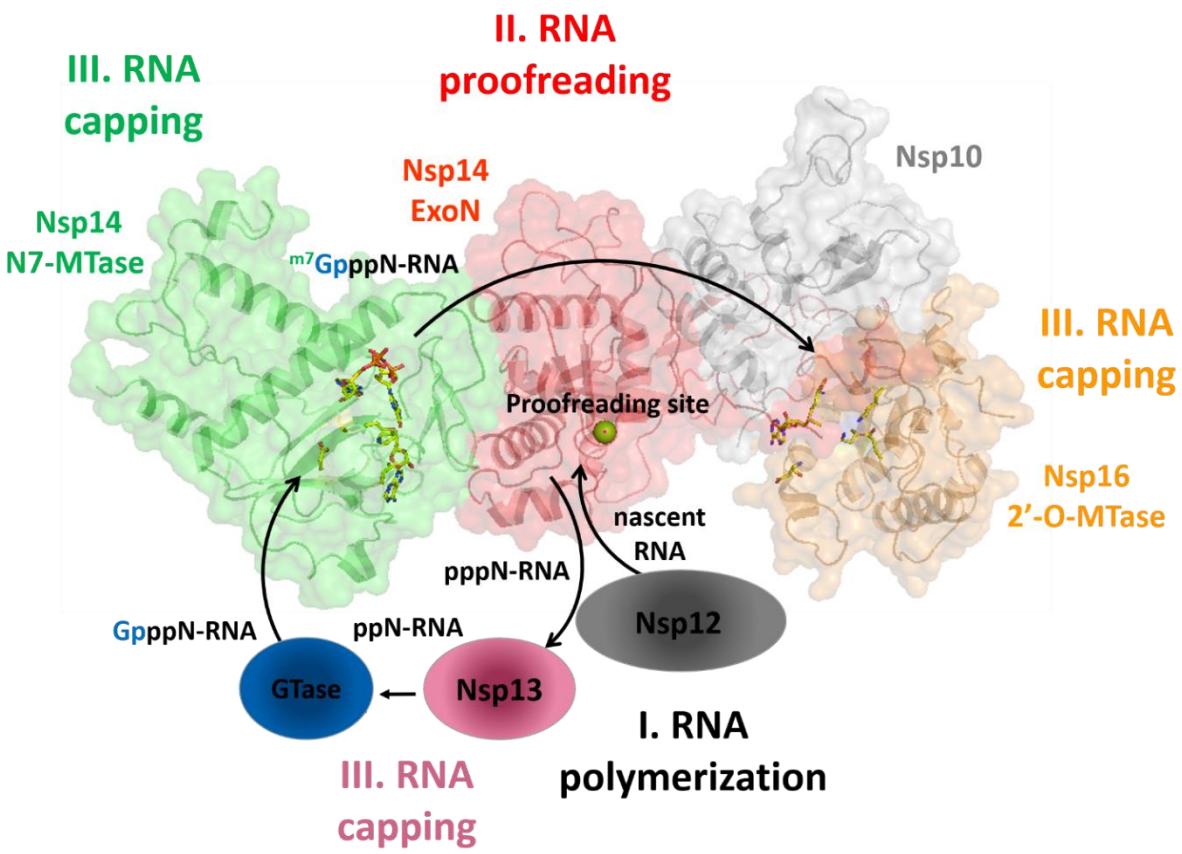

Figure 9. Nsp10 as a molecular connector between proofreading and capping activities. Cartoon and surface representation of the macromolecular complex generated upon superposition of Nsp10 in the two complexes Nsp14-Nsp10 and Nsp16-Nsp10. This model was obtained upon superposition of Nsp10 cofactors of the Nsp10/Nsp14 and Nsp10/Nsp16 complexes. A nascent RNA strand polymerized by Nsp12 (grey oval) is proofread by Nsp14, dephosphorylated by Nsp13 and then capped by GTase, Nsp14 and finally Nsp16.

5. Concluding Remarks

Over the past ten years, we have observed the emergence of many different coronaviruses, causing serious diseases like SARS in 2002, MERS in 2012 and currently COVID19. It is more than likely that these viruses will emerge again in the near future, due to their ability to mutate and attack different hosts, as we have just observed for SARS-CoV-2, which has evolved from a bat disease to a human outbreak. A possible strategy is to identify those processes which are more preserved in all coronaviruses and deeply understand their mechanisms. Inhibiting these processes have a great chance of developing a pancoronaviral therapeutic strategy. As discussed in this review, molecular actors responsible for RNA replication are among most conserved coronaviral proteins and therefore deserve deep understanding of their structural properties. The composition and the structural organization of the replicase complex of SARS-CoV-2 has not been deeply studied, although research in the field is progressing fast. However, lessons come from studies of RNA replication of similar viruses, as reported in this review. These studies, both structural and functional, have identified and described enzymes responsible for RNA polymerization, proofreading and final capping mechanisms to produce a stable RNA filament. However, an important role is also played by cofactors, which mediate protein-protein interactions and thus conduct the orchestra of RNA processing enzymes to improve their efficiencies. Gaining a complete picture of the intricate process of RNA replication of SARS-CoV-2 significantly improves our ability to design therapeutic tools to reduce disease burden.

Supplementary Materials: The following are available online at www.mdpi.com/xxx/s1, Figure S1: Model of SARS-CoV-2 elongation complex, Table S1: Sequence identities of SARS-CoV2 Nsps with homologous proteins.

Author Contributions: Conceptualization, R.B. and A.R.; methodology and software, R.B., M.R. and A.R.; formal analysis, M.R., F.S. and A.R.; data curation, M.R. and R.B.; writing original draft preparation, R.B.; writing review and editing, R.B. and G.M.; supervision, R.B.; funding acquisition, R.B.

Funding: This research was supported by the project 2017SFBFER funded by the Italian MIUR

Acknowledgments: We would like to acknowledge the help of our technical staff, including Maurizio Amendola and Luca De Luca.

Conflicts of Interest: The authors declare no conflict of interest. The funders had no role in the design of the study; in the collection, analyses, or interpretation of data; in the writing of the manuscript, or in the decision to publish the results.

Abbreviations

WHO World Health Organization

PDB Protein Data Bank

SARS Severe acute respiratory syndrome

MERS Middle East respiratory syndrome

EBOV Ebola virus

NIV Nipah virus

RSV Respiratory syncytial virus

EAV Equine arteritis virus

Nsp Non structural protein

RdRP RNA dependent RNA Polymerase

NiRAN Nidovirus RdRp-Associated Nucleotidyltransferase

NTP nucleoside triphosphate

References

1. Zhou, P.; Yang, X.L.; Wang, X.G.; Hu, B.; Zhang, L.; Zhang, W.; Si, H.R.; Zhu, Y.; Li, B.; Huang, C.L., et al. A pneumonia outbreak associated with a new coronavirus of probable bat origin. *Nature* **2020**, *579*, 270-273, doi:10.1038/s41586-020-2012-7.
2. Wu, J.T.; Leung, K.; Leung, G.M. Nowcasting and forecasting the potential domestic and international spread of the 2019-nCoV outbreak originating in Wuhan, China: a modelling study. *Lancet* **2020**, *395*, 689-697, doi:10.1016/S0140-6736(20)30260-9.
3. Lu, R.; Zhao, X.; Li, J.; Niu, P.; Yang, B.; Wu, H.; Wang, W.; Song, H.; Huang, B.; Zhu, N., et al. Genomic characterisation and epidemiology of 2019 novel coronavirus: implications for virus origins and receptor binding. *Lancet* **2020**, *395*, 565-574, doi:10.1016/S0140-6736(20)30251-8.
4. Luan, J.; Lu, Y.; Jin, X.; Zhang, L. Spike protein recognition of mammalian ACE2 predicts the host range and an optimized ACE2 for SARS-CoV-2 infection. *Biochem Biophys Res Commun* **2020**, 10.1016/j.bbrc.2020.03.047, doi:10.1016/j.bbrc.2020.03.047.
5. Wrapp, D.; Wang, N.; Corbett, K.S.; Goldsmith, J.A.; Hsieh, C.L.; Abiona, O.; Graham, B.S.; McLellan, J.S. Cryo-EM structure of the 2019-nCoV spike in the prefusion conformation. *Science* **2020**, *367*, 1260-1263, doi:10.1126/science.abb2507.
6. Wang, K.; Chen, W.; Zhou, Y.-S.; Lian, J.-Q.; Zhang, Z.; Du, P.; Gong, L.; Zhang, Y.; Cui, H.-Y.; Geng, J.-J., et al. SARS-CoV-2 invades host cells via a novel route: CD147-spike protein. *BioRxiv* **2020**.

7. Hoffmann, M.; Kleine-Weber, H.; Schroeder, S.; Krüger, N.; Herrler, T.; Erichsen, S.; Schiergens, T.S.; Herrler, G.; Wu, N.H.; Nitsche, A., et al. SARS-CoV-2 Cell Entry Depends on ACE2 and TMPRSS2 and Is Blocked by a Clinically Proven Protease Inhibitor. *Cell* **2020**, 10.1016/j.cell.2020.02.052, doi:10.1016/j.cell.2020.02.052.
8. Yang, N.; Shen, H.M. Targeting the Endocytic Pathway and Autophagy Process as a Novel Therapeutic Strategy in COVID-19. *Int J Biol Sci* **2020**, *16*, 1724-1731, doi:10.7150/ijbs.45498.
9. Xia, S.; Zhu, Y.; Liu, M.; Lan, Q.; Xu, W.; Wu, Y.; Ying, T.; Liu, S.; Shi, Z.; Jiang, S., et al. Fusion mechanism of 2019-nCoV and fusion inhibitors targeting HR1 domain in spike protein. *Cell Mol Immunol* **2020**, 10.1038/s41423-020-0374-2, doi:10.1038/s41423-020-0374-2.
10. Gordon, D.E.; M. Jang, G.; Bouhaddou, M.; Krogan, N.J. A SARS-CoV-2-Human Protein-Protein Interaction Map Reveals Drug Targets and Potential Drug-Repurposing. *BioXriv* **2020**.
11. Brai, A.; Martelli, F.; Riva, V.; Garbelli, A.; Fazi, R.; Zamperini, C.; Pollutri, A.; Falsitta, L.; Ronzini, S.; Maccari, L., et al. DDX3X Helicase Inhibitors as a New Strategy To Fight the West Nile Virus Infection. *J Med Chem* **2019**, *62*, 2333-2347, doi:10.1021/acs.jmedchem.8b01403.
12. Brai, A.; Fazi, R.; Tintori, C.; Zamperini, C.; Bugli, F.; Sanguinetti, M.; Stigliano, E.; Este, J.; Badia, R.; Franco, S., et al. Human DDX3 protein is a valuable target to develop broad spectrum antiviral agents. *Proc Natl Acad Sci U S A* **2016**, *113*, 5388-5393, doi:10.1073/pnas.1522987113.
13. Wu, A.; Peng, Y.; Huang, B.; Ding, X.; Wang, X.; Niu, P.; Meng, J.; Zhu, Z.; Zhang, Z.; Wang, J., et al. Genome Composition and Divergence of the Novel Coronavirus (2019-nCoV) Originating in China. *Cell Host Microbe* **2020**, *27*, 325-328, doi:10.1016/j.chom.2020.02.001.
14. Gorbalenya, A.E.; Enjuanes, L.; Ziebuhr, J.; Snijder, E.J. Nidovirales: evolving the largest RNA virus genome. *Virus Res* **2006**, *117*, 17-37, doi:10.1016/j.virusres.2006.01.017.
15. Wu, F.; Zhao, S.; Yu, B.; Chen, Y.M.; Wang, W.; Song, Z.G.; Hu, Y.; Tao, Z.W.; Tian, J.H.; Pei, Y.Y., et al. A new coronavirus associated with human respiratory disease in China. *Nature* **2020**, *579*, 265-269, doi:10.1038/s41586-020-2008-3.
16. Cheng, A.; Zhang, W.; Xie, Y.; Jiang, W.; Arnold, E.; Sarafianos, S.G.; Ding, J. Expression, purification, and characterization of SARS coronavirus RNA polymerase. *Virology* **2005**, *335*, 165-176, doi:10.1016/j.virol.2005.02.017.
17. Ivanov, K.A.; Thiel, V.; Dobbe, J.C.; van der Meer, Y.; Snijder, E.J.; Ziebuhr, J. Multiple enzymatic activities associated with severe acute respiratory syndrome coronavirus helicase. *J Virol* **2004**, *78*, 5619-5632, doi:10.1128/JVI.78.11.5619-5632.2004.
18. Feder, M.; Pas, J.; Wyrwicz, L.S.; Bujnicki, J.M. Molecular phylogenetics of the RrmJ/fibrillarin superfamily of ribose 2'-O-methyltransferases. *Gene* **2003**, *302*, 129-138, doi:10.1016/s0378-1119(02)01097-1.
19. Snijder, E.J.; Bredenbeek, P.J.; Dobbe, J.C.; Thiel, V.; Ziebuhr, J.; Poon, L.L.; Guan, Y.; Rozanov, M.; Spaan, W.J.; Gorbalenya, A.E. Unique and conserved features of genome and proteome of SARS-coronavirus, an early split-off from the coronavirus group 2 lineage. *J Mol Biol* **2003**, *331*, 991-1004, doi:10.1016/s0022-2836(03)00865-9.
20. Sevajol, M.; Subissi, L.; Decroly, E.; Canard, B.; Imbert, I. Insights into RNA synthesis, capping, and proofreading mechanisms of SARS-coronavirus. *Virus Res* **2014**, *194*, 90-99, doi:10.1016/j.virusres.2014.10.008.

21. Bhardwaj, K.; Guarino, L.; Kao, C.C. The severe acute respiratory syndrome coronavirus Nsp15 protein is an endoribonuclease that prefers manganese as a cofactor. *J Virol* **2004**, *78*, 12218-12224, doi:10.1128/JVI.78.22.12218-12224.2004.
22. Ivanov, K.A.; Hertzig, T.; Rozanov, M.; Bayer, S.; Thiel, V.; Gorbalenya, A.E.; Ziebuhr, J. Major genetic marker of nidoviruses encodes a replicative endoribonuclease. *Proc Natl Acad Sci U S A* **2004**, *101*, 12694-12699, doi:10.1073/pnas.0403127101.
23. Imbert, I.; Guillemot, J.C.; Bourhis, J.M.; Bussetta, C.; Coutard, B.; Egloff, M.P.; Ferron, F.; Gorbalenya, A.E.; Canard, B. A second, non-canonical RNA-dependent RNA polymerase in SARS coronavirus. *EMBO J* **2006**, *25*, 4933-4942, doi:10.1038/sj.emboj.7601368.
24. Subissi, L.; Posthuma, C.C.; Collet, A.; Zevenhoven-Dobbe, J.C.; Gorbalenya, A.E.; Decroly, E.; Snijder, E.J.; Canard, B.; Imbert, I. One severe acute respiratory syndrome coronavirus protein complex integrates processive RNA polymerase and exonuclease activities. *Proc Natl Acad Sci U S A* **2014**, *111*, E3900-3909, doi:10.1073/pnas.1323705111.
25. Bouvet, M.; Lugari, A.; Posthuma, C.C.; Zevenhoven, J.C.; Bernard, S.; Betzi, S.; Imbert, I.; Canard, B.; Guillemot, J.C.; Lécine, P., et al. Coronavirus Nsp10, a critical co-factor for activation of multiple replicative enzymes. *J Biol Chem* **2014**, *289*, 25783-25796, doi:10.1074/jbc.M114.577353.
26. Knoops, K.; Kikkert, M.; Worm, S.H.; Zevenhoven-Dobbe, J.C.; van der Meer, Y.; Koster, A.J.; Mommaas, A.M.; Snijder, E.J. SARS-coronavirus replication is supported by a reticulovesicular network of modified endoplasmic reticulum. *PLoS Biol* **2008**, *6*, e226, doi:10.1371/journal.pbio.0060226.
27. Angelini, M.M.; Akhlaghpour, M.; Neuman, B.W.; Buchmeier, M.J. Severe acute respiratory syndrome coronavirus nonstructural proteins 3, 4, and 6 induce double-membrane vesicles. *mBio* **2013**, *4*, doi:10.1128/mBio.00524-13.
28. Sawicki, S.G.; Sawicki, D.L.; Siddell, S.G. A contemporary view of coronavirus transcription. *J Virol* **2007**, *81*, 20-29, doi:10.1128/JVI.01358-06.
29. Cameron CE, G.M. Viral Genome Replication. ed Raney K (Springer, New York). 2009.
30. von Brunn, A.; Teepe, C.; Simpson, J.C.; Pepperkok, R.; Friedel, C.C.; Zimmer, R.; Roberts, R.; Baric, R.; Haas, J. Analysis of intraviral protein-protein interactions of the SARS coronavirus ORFeome. *PLoS One* **2007**, *2*, e459, doi:10.1371/journal.pone.0000459.
31. Tan, Y.W.; Fung, T.S.; Shen, H.; Huang, M.; Liu, D.X. Coronavirus infectious bronchitis virus non-structural proteins 8 and 12 form stable complex independent of the non-translated regions of viral RNA and other viral proteins. *Virology* **2018**, *513*, 75-84, doi:10.1016/j.virol.2017.10.004.
32. Jia, Z.; Yan, L.; Ren, Z.; Wu, L.; Wang, J.; Guo, J.; Zheng, L.; Ming, Z.; Zhang, L.; Lou, Z., et al. Delicate structural coordination of the Severe Acute Respiratory Syndrome coronavirus Nsp13 upon ATP hydrolysis. *Nucleic Acids Res* **2019**, *47*, 6538-6550, doi:10.1093/nar/gkz409.
33. Seybert, A.; Posthuma, C.C.; van Dinten, L.C.; Snijder, E.J.; Gorbalenya, A.E.; Ziebuhr, J. A complex zinc finger controls the enzymatic activities of nidovirus helicases. *J Virol* **2005**, *79*, 696-704, doi:10.1128/JVI.79.2.696-704.2005.
34. Lehmann, K.C.; Snijder, E.J.; Posthuma, C.C.; Gorbalenya, A.E. What we know but do not understand about nidovirus helicases. *Virus Res* **2015**, *202*, 12-32, doi:10.1016/j.virusres.2014.12.001.
35. Brockway, S.M.; Clay, C.T.; Lu, X.T.; Denison, M.R. Characterization of the expression, intracellular localization, and replication complex association of the putative mouse hepatitis virus RNA-dependent RNA polymerase. *J Virol* **2003**, *77*, 10515-10527, doi:10.1128/jvi.77.19.10515-10527.2003.

36. Zhang, L.; Li, L.; Yan, L.; Ming, Z.; Jia, Z.; Lou, Z.; Rao, Z. Structural and Biochemical Characterization of Endoribonuclease Nsp15 Encoded by Middle East Respiratory Syndrome Coronavirus. *J Virol* **2018**, *92*, doi:10.1128/JVI.00893-18.

37. Athmer, J.; Fehr, A.R.; Grunewald, M.; Smith, E.C.; Denison, M.R.; Perlman, S. In Situ Tagged nsp15 Reveals Interactions with Coronavirus Replication/Transcription Complex-Associated Proteins. *mBio* **2017**, *8*, doi:10.1128/mBio.02320-16.

38. Deming, D.J.; Graham, R.L.; Denison, M.R.; Baric, R.S. Processing of open reading frame 1a replicase proteins nsp7 to nsp10 in murine hepatitis virus strain A59 replication. *J Virol* **2007**, *81*, 10280-10291, doi:10.1128/JVI.00017-07.

39. Kirchdoerfer, R.N.; Ward, A.B. Structure of the SARS-CoV nsp12 polymerase bound to nsp7 and nsp8 co-factors. *Nat Commun* **2019**, *10*, 2342, doi:10.1038/s41467-019-10280-3.

40. Gao, Y.; Yan, L.; Huang, Y.; Liu, F.; Zhao, Y.; Cao, L.; Wang, T.; Sun, Q.; Ming, Z.; Zhang, L., et al. Structure of the RNA-dependent RNA polymerase from COVID-19 virus. *Science* **2020**, 10.1126/science.abb7498, doi:10.1126/science.abb7498.

41. Lehmann, K.C.; Gulyaeva, A.; Zevenhoven-Dobbe, J.C.; Janssen, G.M.; Ruben, M.; Overkleeft, H.S.; van Veelen, P.A.; Samborskiy, D.V.; Kravchenko, A.A.; Leontovich, A.M., et al. Discovery of an essential nucleotidylating activity associated with a newly delineated conserved domain in the RNA polymerase-containing protein of all nidoviruses. *Nucleic Acids Res* **2015**, *43*, 8416-8434, doi:10.1093/nar/gkv838.

42. Liau, N.P.D.; Laktyushin, A.; Lucet, I.S.; Murphy, J.M.; Yao, S.; Whitlock, E.; Callaghan, K.; Nicola, N.A.; Kershaw, N.J.; Babon, J.J. The molecular basis of JAK/STAT inhibition by SOCS1. *Nat Commun* **2018**, *9*, 1558, doi:10.1038/s41467-018-04013-1.

43. Arnold, J.J.; Cameron, C.E. Poliovirus RNA-dependent RNA polymerase (3D(pol)). Assembly of stable, elongation-competent complexes by using a symmetrical primer-template substrate (sym/sub). *J Biol Chem* **2000**, *275*, 5329-5336, doi:10.1074/jbc.275.8.5329.

44. Arias, A.; Arnold, J.J.; Sierra, M.; Smidansky, E.D.; Domingo, E.; Cameron, C.E. Determinants of RNA-dependent RNA polymerase (in)fidelity revealed by kinetic analysis of the polymerase encoded by a foot-and-mouth disease virus mutant with reduced sensitivity to ribavirin. *J Virol* **2008**, *82*, 12346-12355, doi:10.1128/JVI.01297-08.

45. Yin, W.; Mao, C.; Luan, X.; Shen, D.-D.; Shen, Q.; Su, H.; Wang, X.; Zhou, F.; Zhao, W.; Gao, M., et al. Structural Basis for the Inhibition of the RNA-Dependent RNA Polymerase from SARS-CoV-2 by Remdesivir. *BioXriv* **2020**.

46. Gong, P.; Peersen, O.B. Structural basis for active site closure by the poliovirus RNA-dependent RNA polymerase. *Proc Natl Acad Sci U S A* **2010**, *107*, 22505-22510, doi:10.1073/pnas.1007626107.

47. Warren, T.K.; Jordan, R.; Lo, M.K.; Ray, A.S.; Mackman, R.L.; Soloveva, V.; Siegel, D.; Perron, M.; Bannister, R.; Hui, H.C., et al. Therapeutic efficacy of the small molecule GS-5734 against Ebola virus in rhesus monkeys. *Nature* **2016**, *531*, 381-385, doi:10.1038/nature17180.

48. Agostini, M.L.; Andres, E.L.; Sims, A.C.; Graham, R.L.; Sheahan, T.P.; Lu, X.; Smith, E.C.; Case, J.B.; Feng, J.Y.; Jordan, R., et al. Coronavirus Susceptibility to the Antiviral Remdesivir (GS-5734) Is Mediated by the Viral Polymerase and the Proofreading Exoribonuclease. *mBio* **2018**, *9*, doi:10.1128/mBio.00221-18.

49. Brown, A.J.; Won, J.J.; Graham, R.L.; Dinnon, K.H., 3rd; Sims, A.C.; Feng, J.Y.; Cihlar, T.; Denison, M.R.; Baric, R.S.; Sheahan, T.P. Broad spectrum antiviral remdesivir inhibits human endemic and zoonotic

deltacoronaviruses with a highly divergent RNA dependent RNA polymerase. *Antiviral Res* **2019**, *169*, 104541, doi:10.1016/j.antiviral.2019.104541.

50. Wang, M.; Cao, R.; Zhang, L.; Yang, X.; Liu, J.; Xu, M.; Shi, Z.; Hu, Z.; Zhong, W.; Xiao, G. Remdesivir and chloroquine effectively inhibit the recently emerged novel coronavirus (2019-nCoV) in vitro. *Cell Res* **2020**, *30*, 269-271, doi:10.1038/s41422-020-0282-0.
51. de Wit, E.; Feldmann, F.; Cronin, J.; Jordan, R.; Okumura, A.; Thomas, T.; Scott, D.; Cihlar, T.; Feldmann, H. Prophylactic and therapeutic remdesivir (GS-5734) treatment in the rhesus macaque model of MERS-CoV infection. *Proc Natl Acad Sci U S A* **2020**, 10.1073/pnas.1922083117, doi:10.1073/pnas.1922083117.
52. Lo, M.K.; Jordan, R.; Arvey, A.; Sudhamsu, J.; Shrivastava-Ranjan, P.; Hotard, A.L.; Flint, M.; McMullan, L.K.; Siegel, D.; Clarke, M.O., et al. GS-5734 and its parent nucleoside analog inhibit Filo-, Pneumo-, and Paramyxoviruses. *Sci Rep* **2017**, *7*, 43395, doi:10.1038/srep43395.
53. Sheahan, T.P.; Sims, A.C.; Graham, R.L.; Menachery, V.D.; Gralinski, L.E.; Case, J.B.; Leist, S.R.; Pyrc, K.; Feng, J.Y.; Trantcheva, I., et al. Broad-spectrum antiviral GS-5734 inhibits both epidemic and zoonotic coronaviruses. *Sci Transl Med* **2017**, *9*, doi:10.1126/scitranslmed.aal3653.
54. Sheahan, T.P.; Sims, A.C.; Leist, S.R.; Schafer, A.; Won, J.; Brown, A.J.; Montgomery, S.A.; Hogg, A.; Babusis, D.; Clarke, M.O., et al. Comparative therapeutic efficacy of remdesivir and combination lopinavir, ritonavir, and interferon beta against MERS-CoV. *Nat Commun* **2020**, *11*, 222, doi:10.1038/s41467-019-13940-6.
55. Cardile, A.P.; Warren, T.K.; Martins, K.A.; Reisler, R.B.; Bavari, S. Will There Be a Cure for Ebola? *Annu Rev Pharmacol Toxicol* **2017**, *57*, 329-348, doi:10.1146/annurev-pharmtox-010716-105055.
56. Jordan, P.C.; Liu, C.; Raynaud, P.; Lo, M.K.; Spiropoulou, C.F.; Symons, J.A.; Beigelman, L.; Deval, J. Initiation, extension, and termination of RNA synthesis by a paramyxovirus polymerase. *PLoS Pathog* **2018**, *14*, e1006889, doi:10.1371/journal.ppat.1006889.
57. Tchesnokov, E.P.; Feng, J.Y.; Porter, D.P.; Gotte, M. Mechanism of Inhibition of Ebola Virus RNA-Dependent RNA Polymerase by Remdesivir. *Viruses* **2019**, *11*, doi:10.3390/v11040326.
58. Gordon, C.J.; Tchesnokov, E.P.; Feng, J.Y.; Porter, D.P.; Gotte, M. The antiviral compound remdesivir potently inhibits RNA-dependent RNA polymerase from Middle East respiratory syndrome coronavirus. *J Biol Chem* **2020**, 10.1074/jbc.AC120.013056, doi:10.1074/jbc.AC120.013056.
59. Holshue, M.L.; DeBolt, C.; Lindquist, S.; Lofy, K.H.; Wiesman, J.; Bruce, H.; Spitters, C.; Ericson, K.; Wilkerson, S.; Tural, A., et al. First Case of 2019 Novel Coronavirus in the United States. *N Engl J Med* **2020**, *382*, 929-936, doi:10.1056/NEJMoa2001191.
60. Lai, C.C.; Shih, T.P.; Ko, W.C.; Tang, H.J.; Hsueh, P.R. Severe acute respiratory syndrome coronavirus 2 (SARS-CoV-2) and coronavirus disease-2019 (COVID-19): The epidemic and the challenges. *Int J Antimicrob Agents* **2020**, 10.1016/j.ijantimicag.2020.105924, 105924, doi:10.1016/j.ijantimicag.2020.105924.
61. Ma, Y.; Wu, L.; Shaw, N.; Gao, Y.; Wang, J.; Sun, Y.; Lou, Z.; Yan, L.; Zhang, R.; Rao, Z. Structural basis and functional analysis of the SARS coronavirus nsp14-nsp10 complex. *Proc Natl Acad Sci U S A* **2015**, *112*, 9436-9441, doi:10.1073/pnas.1508686112.
62. Ogando, N.S.; Ferron, F.; Decroly, E.; Canard, B.; Posthuma, C.C.; Snijder, E.J. The Curious Case of the Nidovirus Exoribonuclease: Its Role in RNA Synthesis and Replication Fidelity. *Front Microbiol* **2019**, *10*, 1813, doi:10.3389/fmicb.2019.01813.
63. Becares, M.; Pascual-Iglesias, A.; Nogales, A.; Sola, I.; Enjuanes, L.; Zuniga, S. Mutagenesis of Coronavirus nsp14 Reveals Its Potential Role in Modulation of the Innate Immune Response. *J Virol* **2016**, *90*, 5399-5414, doi:10.1128/JVI.03259-15.

64. Eckerle, L.D.; Lu, X.; Sperry, S.M.; Choi, L.; Denison, M.R. High fidelity of murine hepatitis virus replication is decreased in nsp14 exoribonuclease mutants. *Journal of Virology* **2007**, *81*, 12135-12144, doi:10.1128/Jvi.01296-07.

65. Eckerle, L.D.; Becker, M.M.; Halpin, R.A.; Li, K.; Venter, E.; Lu, X.T.; Scherbakova, S.; Graham, R.L.; Baric, R.S.; Stockwell, T.B., et al. Infidelity of SARS-CoV Nsp14-Exonuclease Mutant Virus Replication Is Revealed by Complete Genome Sequencing. *Plos Pathog* **2010**, *6*, doi:ARTN e1000896 10.1371/journal.ppat.1000896.

66. Marcotrigiano, J.; Gingras, A.C.; Sonenberg, N.; Burley, S.K. Cocrystal structure of the messenger RNA 5' cap-binding protein (eIF4E) bound to 7-methyl-GDP. *Cell* **1997**, *89*, 951-961, doi:Doi 10.1016/S0092-8674(00)80280-9.

67. Decroly, E.; Ferron, F.; Lescar, J.; Canard, B. Conventional and unconventional mechanisms for capping viral mRNA. *Nat Rev Microbiol* **2012**, *10*, 51-65, doi:10.1038/nrmicro2675.

68. Ferron, F.; Subissi, L.; De Morais, A.T.S.; Le, N.T.T.; Sevajol, M.; Gluais, L.; Decroly, E.; Vonrhein, C.; Bricogne, G.; Canard, B., et al. Structural and molecular basis of mismatch correction and ribavirin excision from coronavirus RNA. *P Natl Acad Sci USA* **2018**, *115*, E162-E171, doi:10.1073/pnas.1718806115.

69. Bouvet, M.; Imbert, I.; Subissi, L.; Gluais, L.; Canard, B.; Decroly, E. RNA 3 '-end mismatch excision by the severe acute respiratory syndrome coronavirus nonstructural protein nsp10/nsp14 exoribonuclease complex. *P Natl Acad Sci USA* **2012**, *109*, 9372-9377, doi:10.1073/pnas.1201130109.

70. Derbyshire, V.; Grindley, N.D.F.; Joyce, C.M. The 3'-5' Exonuclease of DNA-Polymerase-I of Escherichia-Coli - Contribution of Each Amino-Acid at the Active-Site to the Reaction. *Embo J* **1991**, *10*, 17-24, doi:DOI 10.1002/j.1460-2075.1991.tb07916.x.

71. Romano, M.; Squeglia, F.; Berisio, R. Structure and Function of RNase AS: A Novel Virulence Factor From Mycobacterium tuberculosis. *Curr Med Chem* **2015**, *22*, 1745-1756, doi:Doi 10.2174/0929867322666150417125301.

72. Romano, M.; van de Weerd, R.; Brouwer, F.C.; Roviello, G.N.; Lacroix, R.; Sparrius, M.; van den Brink-van Stempvoort, G.; Maaskant, J.J.; van der Sar, A.M.; Appelmelk, B.J., et al. Structure and function of RNase AS, a polyadenylate-specific exoribonuclease affecting mycobacterial virulence in vivo. *Structure* **2014**, *22*, 719-730, doi:10.1016/j.str.2014.01.014.

73. Minskaia, E.; Hertzig, T.; Gorbalenya, A.E.; Campanacci, V.; Cambillau, C.; Canard, B.; Ziebuhr, J. Discovery of an RNA virus 3 '-> 5 ' exoribonuclease that is critically involved in coronavirus RNA synthesis. *P Natl Acad Sci USA* **2006**, *103*, 5108-5113, doi:10.1073/pnas.0508200103.

74. Calvanese, L.; Squeglia, F.; Romano, M.; D'Auria, G.; Falcigno, L.; Berisio, R. Structural and dynamic studies provide insights into specificity and allosteric regulation of ribonuclease as, a key enzyme in mycobacterial virulence. *J Biomol Struct Dyn* **2019**, 10.1080/07391102.2019.1643786, 1-13, doi:10.1080/07391102.2019.1643786.

75. Denison, M.R.; Graham, R.L.; Donaldson, E.F.; Eckerle, L.D.; Baric, R.S. Coronaviruses An RNA proofreading machine regulates replication fidelity and diversity. *Rna Biol* **2011**, *8*, 270-279, doi:10.4161/rna.8.2.15013.

76. Tchesnokov, E.P.; Obikhod, A.; Schinazi, R.F.; Gotte, M. Delayed chain termination protects the anti-hepatitis B virus drug entecavir from excision by HIV-1 reverse transcriptase. *J Biol Chem* **2008**, *283*, 34218-34228, doi:10.1074/jbc.M806797200.

77. Dulin, D.; Arnold, J.J.; van Laar, T.; Oh, H.S.; Lee, C.; Perkins, A.L.; Harki, D.A.; Depken, M.; Cameron, C.E.; Dekker, N.H. Signatures of Nucleotide Analog Incorporation by an RNA-Dependent RNA

Polymerase Revealed Using High-Throughput Magnetic Tweezers. *Cell Rep* **2017**, *21*, 1063-1076, doi:10.1016/j.celrep.2017.10.005.

78. Smith, E.C.; Blanc, H.; Surdel, M.C.; Vignuzzi, M.; Denison, M.R. Coronaviruses lacking exoribonuclease activity are susceptible to lethal mutagenesis: evidence for proofreading and potential therapeutics. *PLoS Pathog* **2013**, *9*, e1003565, doi:10.1371/journal.ppat.1003565.
79. Morse, J.S.; Lalonde, T.; Xu, S.; Liu, W.R. Learning from the Past: Possible Urgent Prevention and Treatment Options for Severe Acute Respiratory Infections Caused by 2019-nCoV. *Chembiochem* **2020**, *21*, 730-738, doi:10.1002/cbic.202000047.
80. Rao, S.T.; Rossmann, M.G. Comparison of super-secondary structures in proteins. *J Mol Biol* **1973**, *76*, 241-256, doi:10.1016/0022-2836(73)90388-4.
81. Byszewska, M.; Smietanski, M.; Purta, E.; Bujnicki, J.M. RNA methyltransferases involved in 5' cap biosynthesis. *Rna Biol* **2014**, *11*, 1597-1607, doi:10.1080/15476286.2015.1004955.
82. Chouhan, B.P.S.; Maimaiti, S.; Gade, M.; Laurino, P. Rossmann-Fold Methyltransferases: Taking a "beta-Turn" around Their Cofactor, S-Adenosylmethionine. *Biochemistry-Us* **2019**, *58*, 166-170, doi:10.1021/acs.biochem.8b00994.
83. Schubert, H.L.; Blumenthal, R.M.; Cheng, X.D. Many paths to methyltransfer: a chronicle of convergence. *Trends Biochem Sci* **2003**, *28*, 329-335, doi:10.1016/S0968-0004(03)00090-2.
84. Chen, Y.; Cai, H.; Pan, J.; Xiang, N.; Tien, P.; Ahola, T.; Guo, D.Y. Functional screen reveals SARS coronavirus nonstructural protein nsp14 as a novel cap N7 methyltransferase. *P Natl Acad Sci USA* **2009**, *106*, 3484-3489, doi:10.1073/pnas.0808790106.
85. Chen, Y.; Tao, J.L.; Sun, Y.; Wu, A.D.; Su, C.Y.; Gao, G.Z.; Cai, H.; Qiu, S.; Wu, Y.L.; Ahola, T., et al. Structure-Function Analysis of Severe Acute Respiratory Syndrome Coronavirus RNA Cap Guanine-N7-Methyltransferase. *Journal of Virology* **2013**, *87*, 6296-6305, doi:10.1128/Jvi.00061-13.
86. Jin, X.; Chen, Y.; Sun, Y.; Zeng, C.; Wang, Y.; Tao, J.L.; Wu, A.D.; Yu, X.; Zhang, Z.; Tian, J., et al. Characterization of the guanine-N7 methyltransferase activity of coronavirus nsp14 on nucleotide GTP. *Virus Research* **2013**, *176*, 45-52, doi:10.1016/j.virusres.2013.05.001.
87. Chen, Y.; Su, C.Y.; Ke, M.; Jin, X.; Xu, L.R.; Zhang, Z.; Wu, A.D.; Sun, Y.; Yang, Z.N.; Tien, P., et al. Biochemical and Structural Insights into the Mechanisms of SARS Coronavirus RNA Ribose 2 '-O-Methylation by nsp16/nsp10 Protein Complex. *Plos Pathog* **2011**, *7*, doi:ARTN e1002294 10.1371/journal.ppat.1002294.
88. Decroly, E.; Debarnot, C.; Ferron, F.; Bouvet, M.; Coutard, B.; Imbert, I.; Gluais, L.; Papageorgiou, N.; Sharff, A.; Bricogne, G., et al. Crystal Structure and Functional Analysis of the SARS-Coronavirus RNA Cap 2 '-O-Methyltransferase nsp10/nsp16 Complex. *Plos Pathog* **2011**, *7*, doi:ARTN e1002059 10.1371/journal.ppat.1002059.
89. Jankowsky, E.; Fairman, M.E. RNA helicases--one fold for many functions. *Curr Opin Struct Biol* **2007**, *17*, 316-324, doi:10.1016/j.sbi.2007.05.007.
90. Deng, Z.; Lehmann, K.C.; Li, X.; Feng, C.; Wang, G.; Zhang, Q.; Qi, X.; Yu, L.; Zhang, X.; Feng, W., et al. Structural basis for the regulatory function of a complex zinc-binding domain in a replicative arterivirus helicase resembling a nonsense-mediated mRNA decay helicase. *Nucleic Acids Res* **2014**, *42*, 3464-3477, doi:10.1093/nar/gkt1310.
91. Ivanov, K.A.; Ziebuhr, J. Human coronavirus 229E nonstructural protein 13: characterization of duplex-unwinding, nucleoside triphosphatase, and RNA 5'-triphosphatase activities. *J Virol* **2004**, *78*, 7833-7838, doi:10.1128/JVI.78.14.7833-7838.2004.

92. Adedeji, A.O.; Lazarus, H. Biochemical Characterization of Middle East Respiratory Syndrome Coronavirus Helicase. *mSphere* **2016**, *1*, doi:10.1128/mSphere.00235-16.

93. Adedeji, A.O.; Marchand, B.; Te Velthuis, A.J.; Snijder, E.J.; Weiss, S.; Eoff, R.L.; Singh, K.; Sarafianos, S.G. Mechanism of nucleic acid unwinding by SARS-CoV helicase. *PLoS One* **2012**, *7*, e36521, doi:10.1371/journal.pone.0036521.

94. Ziebuhr, J. The coronavirus replicase. *Curr Top Microbiol Immunol* **2005**, *287*, 57-94, doi:10.1007/3-540-26765-4_3.

95. van Dinten, L.C.; van Tol, H.; Gorbalenya, A.E.; Snijder, E.J. The predicted metal-binding region of the arterivirus helicase protein is involved in subgenomic mRNA synthesis, genome replication, and virion biogenesis. *J Virol* **2000**, *74*, 5213-5223, doi:10.1128/jvi.74.11.5213-5223.2000.

96. Adedeji, A.O.; Singh, K.; Calcaterra, N.E.; DeDiego, M.L.; Enjuanes, L.; Weiss, S.; Sarafianos, S.G. Severe acute respiratory syndrome coronavirus replication inhibitor that interferes with the nucleic acid unwinding of the viral helicase. *Antimicrob Agents Chemother* **2012**, *56*, 4718-4728, doi:10.1128/AAC.00957-12.

97. Adedeji, A.O.; Singh, K.; Kassim, A.; Coleman, C.M.; Elliott, R.; Weiss, S.R.; Frieman, M.B.; Sarafianos, S.G. Evaluation of SSYA10-001 as a replication inhibitor of severe acute respiratory syndrome, mouse hepatitis, and Middle East respiratory syndrome coronaviruses. *Antimicrob Agents Chemother* **2014**, *58*, 4894-4898, doi:10.1128/AAC.02994-14.

98. Hao, W.; Wojdyla, J.A.; Zhao, R.; Han, R.; Das, R.; Zlatev, I.; Manoharan, M.; Wang, M.; Cui, S. Crystal structure of Middle East respiratory syndrome coronavirus helicase. *PLoS Pathog* **2017**, *13*, e1006474, doi:10.1371/journal.ppat.1006474.

99. Aouadi, W.; Blanjoie, A.; Vasseur, J.J.; Debart, F.; Canard, B.; Decroly, E. Binding of the Methyl Donor S-Adenosyl-L-Methionine to Middle East Respiratory Syndrome Coronavirus 2 '-O-Methyltransferase nsp16 Promotes Recruitment of the Allosteric Activator nsp10. *Journal of Virology* **2017**, *91*, doi:UNSP e02217-16

10.1128/JVI.02217-16.

100. Martin, J.L.; McMillan, F.M. SAM (dependent) I AM: the S-adenosylmethionine-dependent methyltransferase fold. *Curr Opin Struc Biol* **2002**, *12*, 783-793, doi:Doi 10.1016/S0959-440x(02)00391-3.

101. Joseph, J.S.; Saikatendu, K.S.; Subramanian, V.; Neuman, B.W.; Brooun, A.; Griffith, M.; Moy, K.; Yadav, M.K.; Velasquez, J.; Buchmeier, M.J., et al. Crystal structure of nonstructural protein 10 from the severe acute respiratory syndrome coronavirus reveals a novel fold with two zinc-binding motifs. *Journal of Virology* **2006**, *80*, 7894-7901, doi:10.1128/Jvi.00467-06.

102. Su, D.; Lou, Z.Y.; Sun, F.; Zhai, Y.J.; Yang, H.T.; Zhang, R.G.; Joachimiak, A.; Zhang, X.J.C.; Bartlam, M.; Rao, Z.H. Dodecamer structure of severe acute respiratory syndrome coronavirus nonstructural protein nsp10. *Journal of Virology* **2006**, *80*, 7902-7908, doi:10.1128/Jvi.00483-06.

103. Matthes, N.; Mesters, J.R.; Coutard, B.; Canard, B.; Snijder, E.J.; Moll, R.; Hilgenfeld, R. The non-structural protein Nsp10 of mouse hepatitis virus binds zinc ions and nucleic acids. *Febs Lett* **2006**, *580*, 4143-4149, doi:10.1016/j.febslet.2006.06.061.

104. Peti, W.; Johnson, M.A.; Herrmann, T.; Neuman, B.W.; Buchmeier, M.J.; Nelson, M.; Joseph, J.; Page, R.; Stevens, R.C.; Kuhn, P., et al. Structural genomics of the severe acute respiratory syndrome coronavirus: nuclear magnetic resonance structure of the protein nsP7. *J Virol* **2005**, *79*, 12905-12913, doi:10.1128/JVI.79.20.12905-12913.2005.

105. Johnson, M.A.; Jaudzems, K.; Wüthrich, K. NMR Structure of the SARS-CoV Nonstructural Protein 7 in Solution at pH 6.5. *J Mol Biol* **2010**, *402*, 619-628, doi:10.1016/j.jmb.2010.07.043.

106. Zhai, Y.; Sun, F.; Li, X.; Pang, H.; Xu, X.; Bartlam, M.; Rao, Z. Insights into SARS-CoV transcription and replication from the structure of the nsp7-nsp8 hexadecamer. *Nat Struct Mol Biol* **2005**, *12*, 980-986, doi:10.1038/nsmb999.

107. Littler, D.R.; Gully, B.S.; Colson, R.N.; Rossjohn, J. Crystal structure of the SARS-CoV-2 non-structural protein 9, Nsp9. *BioXriv* **2020**.

108. Egloff, M.P.; Ferron, F.; Campanacci, V.; Longhi, S.; Rancurel, C.; Dutartre, H.; Snijder, E.J.; Gorbalenya, A.E.; Cambillau, C.; Canard, B. The severe acute respiratory syndrome-coronavirus replicative protein nsp9 is a single-stranded RNA-binding subunit unique in the RNA virus world. *Proc Natl Acad Sci U S A* **2004**, *101*, 3792-3796, doi:10.1073/pnas.0307877101.

109. Sutton, G.; Fry, E.; Carter, L.; Sainsbury, S.; Walter, T.; Nettleship, J.; Berrow, N.; Owens, R.; Gilbert, R.; Davidson, A., et al. The nsp9 replicase protein of SARS-coronavirus, structure and functional insights. *Structure* **2004**, *12*, 341-353, doi:10.1016/j.str.2004.01.016.

110. Kim, Y.; Jedrzejczak, R.; Maltseva, N.I.; Michael Endres; Adam Godzik; Karolina Michalska; Joachimiak, A. Crystal structure of Nsp15 endoribonuclease NendoU from SARS-CoV-2. *BioXriv* **2020**.

111. Ricagno, S.; Egloff, M.P.; Ulferts, R.; Coutard, B.; Nurizzo, D.; Campanacci, V.; Cambillau, C.; Ziebuhr, J.; Canard, B. Crystal structure and mechanistic determinants of SARS coronavirus nonstructural protein 15 define an endoribonuclease family. *Proc Natl Acad Sci U S A* **2006**, *103*, 11892-11897, doi:10.1073/pnas.0601708103.

112. Bhardwaj, K.; Palaninathan, S.; Alcantara, J.M.; Yi, L.L.; Guarino, L.; Sacchettini, J.C.; Kao, C.C. Structural and functional analyses of the severe acute respiratory syndrome coronavirus endoribonuclease Nsp15. *J Biol Chem* **2008**, *283*, 3655-3664, doi:10.1074/jbc.M708375200.